Volume 18 | Number 5 | 7 February 2016 | Pages 3363–4224

PCCP

Physical Chemistry Chemical Physics

www.rsc.org/pccp

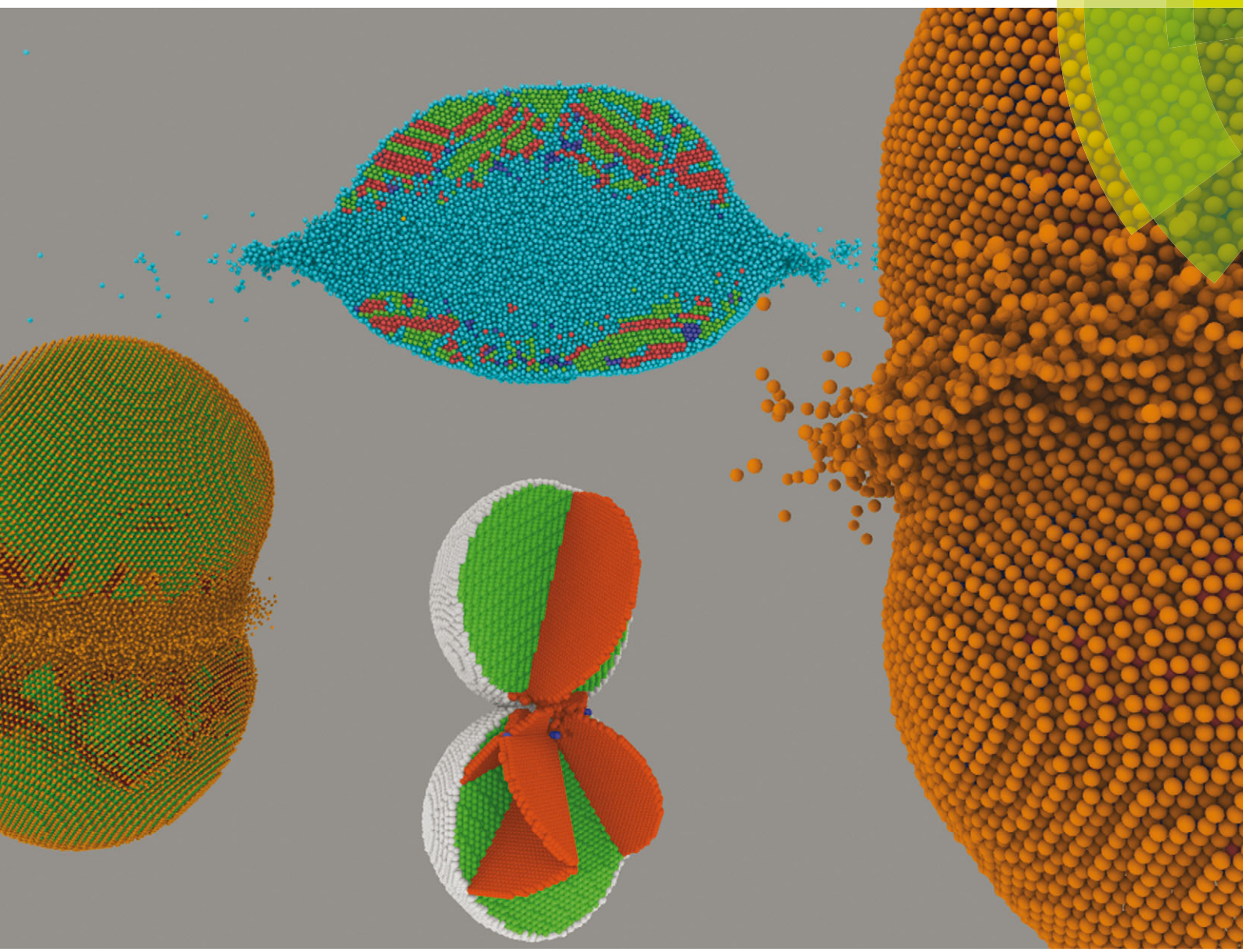

ISSN 1463-9076

ROYAL SOCIETY OF CHEMISTRY

PAPER

Herbert M. Urbassek *et al.*

The elastic–plastic transition in nanoparticle collisions

175 YEARS

PCCP

PAPER

View Article Online
View Journal | View Issue

Cite this: *Phys. Chem. Chem. Phys.*, 2016, **18**, 3423

The elastic–plastic transition in nanoparticle collisions

Emmanuel N. Millán,[a] Diego R. Tramontina,[ab] Herbert M. Urbassek*[c] and Eduardo M. Bringa[a]

Received 28th August 2015,
Accepted 5th October 2015

DOI: 10.1039/c5cp05150a

www.rsc.org/pccp

When nanoparticles (NPs) collide with low velocities, they interact elastically in the sense that – besides their fusion caused by their mutual van-der-Waals attraction – no defects are generated. We investigate the minimum velocity, v_c, necessary for generating defects and inducing plasticity in the NP. The determination of this elastic–plastic threshold is of prime importance for modeling the behavior of granular matter. Using the generic Lennard-Jones interaction potential, we find v_c to increase strongly with decreasing radius. Current models do not agree with our simulations, but we provide a model based on dislocation emission in the contact zone that quantitatively describes the size dependence of the elastic–plastic transition.

I. Introduction

Colliding nanoparticles (NPs) interact at small impact velocities elastically while plastic deformation occurs at larger velocities. The critical velocity, v_c, which separates these two regimes is of prime importance for modeling the consequences of the impact; it is a basic ingredient to all discrete-element models that treat granular collisions on a mesoscopic scale,[1–4] since plastic processes provide a novel route of dissipation of collision energy not present in the elastic regime. The elastic–plastic limit is decisive in such diverse areas as in materials processing of granular matter[5] and dust collisions in astrophysical contexts, such as debris disks and protoplanetary disk atmospheres.[6,7] Experimentally, the determination of v_c is not easy, and experimenters prefer to determine the restitution coefficient or the bouncing velocity (the smallest velocity required for a NP to bounce off a wall rather than to stick to it); they then refer these quantities or changes therein to v_c.

Early estimates of v_c assume this quantity to depend only on the mass density, the plastic yield strength and the elastic moduli.[8,9] v_c was therefore assumed to be independent of the NP size, apart form the fact that the yield strength itself may increase for small NPs due to confinement effects. However, recently it has become possible for experiments to directly explore NPs under load. Thus it was shown that the elastic properties of NPs are basically the same as the bulk elastic properties in the case of Al NPs,[10] but may deviate strongly in the case of Au or Ag NPs.[11,12] Plasticity, on the other hand, can be significantly different at the nanoscale. Plastic deformation in nanoscale systems is being studied in a variety of conditions such as under nanoindentation,[13,14] in nanopillars,[15] nanowhiskers,[16] nanoclusters,[17,18] or in adhesive contacts,[19] and it is often related to plasticity of nanograins in polycrystals,[20] or plasticity arising from nanoscale defects like nanovoids.[21,22] Recent microscopy techniques allow to view dislocations, stacking faults and twins in sub-10 nm NPs.[23] To give but two examples of recent findings, experiments by Zheng *et al.*[24] demonstrate that partial dislocations emitted from the surface dominate plasticity in sub-10 nm Au NPs, and Chrobak *et al.*[14] point at a change of the mechanism of plasticity from a phase-transition to a dislocation-dominated regime in Si.

Complementary to experiments, molecular dynamics (MD) simulation provides a method to determine the processes occurring in NPs at the atomistic scale. Because of the simplicity of the setup, NP collisions have been frequently studied, and results on the restitution coefficient,[25] NP bouncing off a surface or off other NPs,[26,27] grain mixing,[28] fragmentation,[29,30] and the occurrence of inelastic processes[31] have been reported. An analysis of the dislocation generation has been lacking up to now, with the exception of Han *et al.*[32] who explored the interplay of collision inelasticity and dislocation generation by studying the reflection of NPs off a rigid wall.

In this paper we study the onset of plasticity in NP collisions and set up a correlation between NP size and the critical velocity for plastic yield, v_c.

II. Method

We employ a generic interatomic interaction potential, the Lennard-Jones (LJ) potential, which has been frequently used

[a] *CONICET and Facultad de Ciencias Exactas y Naturales, Universidad Nacional de Cuyo, Mendoza, 5500 Argentina*
[b] *Instituto de Bioingeniería, Universidad de Mendoza, Mendoza, M5502BZ Argentina*
[c] *Physics Department and Research Center OPTIMAS, University Kaiserslautern, Erwin-Schrödinger-Straße, D-67663 Kaiserslautern, Germany. E-mail: urbassek@rhrk.uni-kl.de; Web: http://www.physik.uni-kl.de/urbassek/*

Table 1 LJ parameters, ε and σ, and mass, m, for three materials: Ar,[33,34] water,[35,36] and Ag.[37,38] LJ units for velocity, $\bar{v} = \sqrt{\varepsilon/m}$, time $\bar{t} = \sigma\sqrt{m/\varepsilon}$, temperature, $T = \varepsilon/k_B$, and pressure, $\bar{p} = \varepsilon/\sigma^3$, where k_B is Boltzmann's constant

	ε (meV)	σ (Å)	m (amu)	$\bar{v}$ (m s^{-1})	$\bar{t}$ (ps)	$\bar{T}$ (K)	$\bar{p}$ (MPa)
Ar	10.32	3.41	39.95	158	2.16	119.8	41.6
H_2O	30.7	2.725	18.02	404	0.675	358.4	242.7
Ag	345	2.644	107.87	555	0.476	4028	2986

in the past to model NP collisions.[25–27,29,31] The plastic behavior of LJ solids has been thoroughly studied, in particular under shock loading and the dislocation activity in LJ solids has been found to be typical of that of fcc crystals.[1,39,40] LJ potentials are characterized by their well depth ε and the length parameter σ. The potential is cut-off at $r_c = 2.5\sigma$. Data will be reported in reduced LJ units. Table 1 specifies these units for three materials: Ar, water and Ag. The NPs are built by carving spheres of radius R from a perfect fcc structure. The number of atoms, N, in a NP is connected to its radius by $R = 0.607 \times N^{1/3}$ or $N = 4.47 \times R^3$. We study NPs in the range of $N = 10^3$ to 10^6, equivalent to $R = 6.1$ to 61. Here we focus on central (collinear) collisions between identical NPs. The relative orientation between the colliding NPs has been varied; the quantitative results shown are averages of up to 1000 orientations.

The molecular dynamics code LAMMPS[41] is used to perform the simulations. We employ a time step of 0.001. The simulations are carried out in the constant energy ensemble, for an initial temperature of $T = 0.1$. The NPs are started to undergo a central collision with initial relative velocity v. We pursue the simulations for more than 10^5 time steps (equivalent to a final time beyond 100 in LJ units) to ensure a reasonable relaxation of the grains after their collision. VMD (visual molecular dynamics)[42] and OVITO[43] are used to view the simulation results. The generated defects are tracked using the dislocation extraction algorithm (DXA)[44,45] and the crystal analysis tool (CAT).[46]

III. Results

Fig. 1 gives an overview over the processes that occur upon the collision of 2 identical NPs. Here the colors cyan and pink characterize from which NP atoms originate and thus allow to identify the amount of atom transfer (mixing) during the collision. The defects produced by the large stress in the contact area are partial dislocations.[47] They travel rapidly through the NPs such that at the end of the collision, when the snapshots of Fig. 1 are taken, they already swept through the entire NP. Thus the dislocations have actually vanished from the NPs but left behind the trace of their glide through the crystal: steps at the surface – clearly seen for instance in Fig. 1(c) – and a changed sequence of lattice planes in the crystal interior, called stacking faults (SFs). Such SF planes appear prominently in golden color in Fig. 1. If several SFs are produced in consecutive planes, a nanotwin is formed, such as that seen in Fig. 1(c). For certain events around v_c, we observe production of transient SFs which do not reach the opposite surface, and can be reabsorbed leaving defect-free grains at the end of the simulation, as noted before.[30,32]

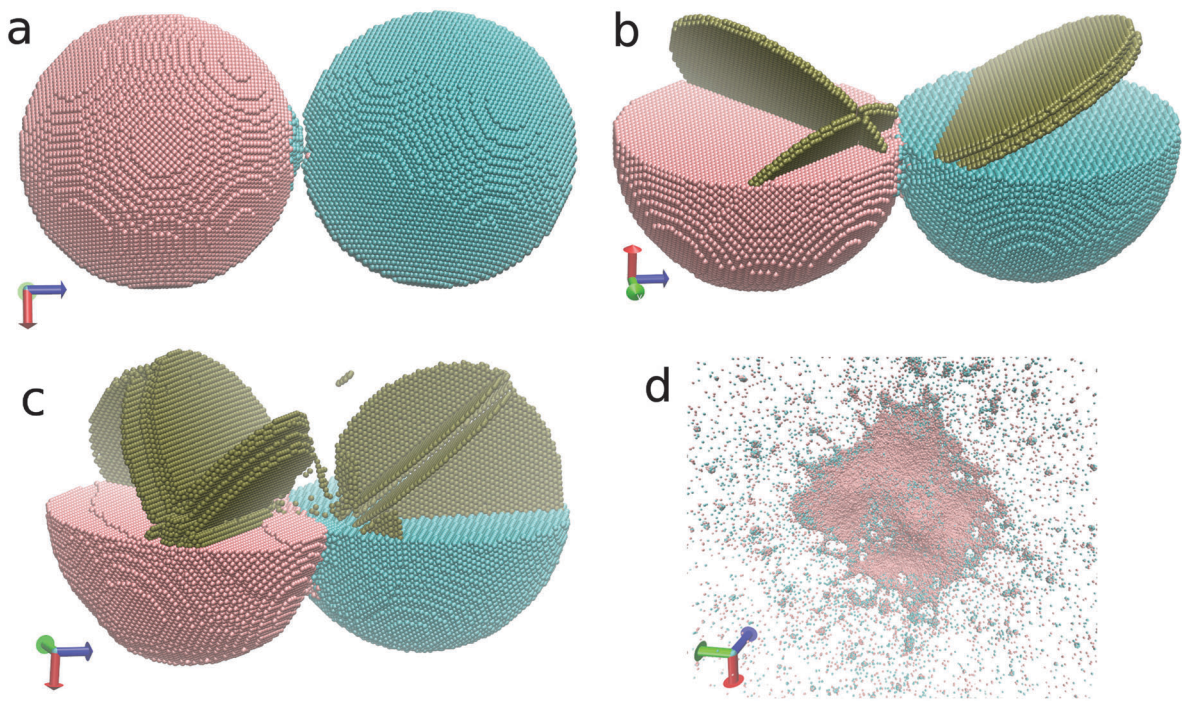

Fig. 1 Synopsis of events occurring in the collision of two NPs ($R = 28.2$, each containing $N = 10^5$ atoms) with velocity (a) $v = 0.2$, (b) $v = 0.5$, (c) $v = 1.0$, (d) $v = 7.0$. While event (a) is elastic with some atomic mixing occurring at the contact region, the cut hemispheres show the development of planar defects in (b), additional localized defects in (c), and NP fragmentation in (d). Colors cyan and pink denote the NP from which atoms originate; defects are in golden color.

Fig. 1 demonstrates that at small velocity, the NPs merely stick together, as the collision energy is dissipated by excitation of phonons and creation of heat; the attractive forces then do not allow the 2 NPs to separate again. At higher velocity, the pressure created in the contact area is large enough to create dislocations; these lead to the SF planes characterizing the induced defects. Clearly their orientation is dictated by the crystallography of the 2 NPs. At still higher velocity, abundant plasticity has been created – showing up in the intersecting SF planes, Fig. 1(c), that originated by dislocations moving along various glide systems – that virtually fills out the entire volume of the NP. Finally, at the largest velocity the 2 NPs are shattered and besides several larger fragments, a large number of monomers have been created.

We note that we occasionally do see bouncing of the 2 NPs; it occurs around v_c, when the velocity is high enough to allow the 2 NPs to separate again after the collision but small enough that plasticity does not yet dominate energy dissipation.[26]

A. Plasticity at the threshold

Fig. 2 shows the atomistic structure of defects formed around the critical velocity. For 4 different NP sizes – varying from $N = 10^3$ to 10^6 – collision velocities slightly above and below the respective v_c were chosen and typical defect structures are shown. Again the colors pink and cyan differentiate between the 2 NPs from which the atoms originate. Here defect atoms are not shown in golden color but in the color of the NP they belong to. While below the critical velocity, only embryonic features are seen – amorphous or plate-like strongly constrained structures – above v_c full SF platelets spanning the entire NP have formed. This demonstrates that already slightly above v_c plasticity is characterized by the formation of volume-spanning planar defects. Dislocations generally nucleate directly at the contact area; from there they expand until they span the entire NP. In Fig. 2(c) it is seen that the formation of planar defects is accompanied by slip leading to steps on the surface. Note that the number of defects generated in the two colliding NPs can differ strongly; this underlines the importance of the NP orientation on the creation of crystal defects.

B. Existing models for critical velocity

We extract the critical velocity v_c from our series of simulations by using the criterion that the number of defect atoms has reached a level of 0.5% of the total number of atoms in the NPs. For the two smallest cluster sizes used here, a threshold of 5% was used instead. In all cases, these criteria agree with the rapid rise in the curves of defects *versus* velocity for a given radius. Our data are averages of collisions using different NP orientations for each radius. A large variation exists in the number of defects generated in NPs of the same R and v if the crystalline orientations of the 2 colliding NPs are different, but 10–100 different orientations are enough to provide a stable mean and standard deviation, and going to 1000 events did not change our results even for the smallest clusters. The data are displayed in Fig. 3 and show that for large NPs v_c levels off at 0.1, while it increases strongly with decreasing sphere radius, reaching $v_c = 0.55$ for the smallest NPs studied, $R = 3.9$.

The critical velocity for plasticity in the collision between two crystalline NPs is highly orientation-dependent, since it is related to the critical resolved shear stress in glide planes. In this study, a large number of collision orientations has been considered to average out this effect; the averaging is analogous to what happens in NP collision experiments due to the difficulty of tuning collision orientations at the nanoscale. This orientation dependence leads to a considerable spread in the number of defects for a given velocity and radius; for velocities in the vicinity of v_c the standard deviation of the defect distribution amounts to around 50% of the average value. However, due to our large number of simulations the error of the average value in v_c reduces to only around 10%. We note that there are certain experimental settings where cluster orientation could become important – such as the compression of NPs of well controlled orientation[48] – and this might lead to different estimates of the critical stress for plasticity initiation.

There are only few models available in the literature that discuss the elastic–plastic transition in NP collisions. The oldest and most often used model predicts v_c to show no explicit dependence on size.[8,9,49,50] For two equal spheres it reads

$$v_c = 10.06\sqrt{\frac{Y^5}{E_{ind}{}^4\rho}}, \quad (1)$$

where Y is the yield stress, $E_{ind} = E/(1 - \nu^2)$ is the indentation modulus, E and ν are Young's modulus and Poisson ratio for the material assumed to be isotropic, and ρ is the mass density. While v_c does not exhibit any explicit size dependence, it has of course been reasoned that the materials properties – and here in particular the yield strength – may depend on size, leading to an increase of v_c for smaller NPs. In our simulations, however, we consider defect-free single-crystalline NPs, so that the materials constants can be assumed to be size independent to a good approximation. Furthermore, we note that due to the small size of the NPs the collisions occur at a high strain rate, $\dot{\varepsilon} \sim v/R$, which may reach values of up to 0.1 for our smallest NPs. While materials constants, and in particular the yield strength Y, do depend on $\dot{\varepsilon}$, this dependence cannot explain any R dependence of the critical velocity, since $\dot{\varepsilon}$ does not change significantly at the contact interface in the NP collisions considered here. In addition we will use the theoretical strength for Y, which provides a reasonable upper bound also at high strain rates.

Quesnel *et al.*[51] calculated for a LJ fcc solid a density of $\rho = 1.08485$. In the same paper they recommend isotropic values for the elastic properties – as determined from an appropriate averaging over the elastic constants – of $E = 100$ and $\nu = 0.25$, resulting in $E_{ind} = 107$. For further use, we note that the shear modulus is $G = 40$ and the bulk modulus is $K = 67$. Taking $Y = G/10 = 4$ for a defect-free single crystal,[52] eqn (1) gives $v_c = 0.027$. This is considerably smaller than our MD results, even for the largest NPs studied here. We note, however, that in a recent study of LJ NPs oriented such that they meet with their (100) facets Takato *et al.*[27] found a larger macroscopic value of

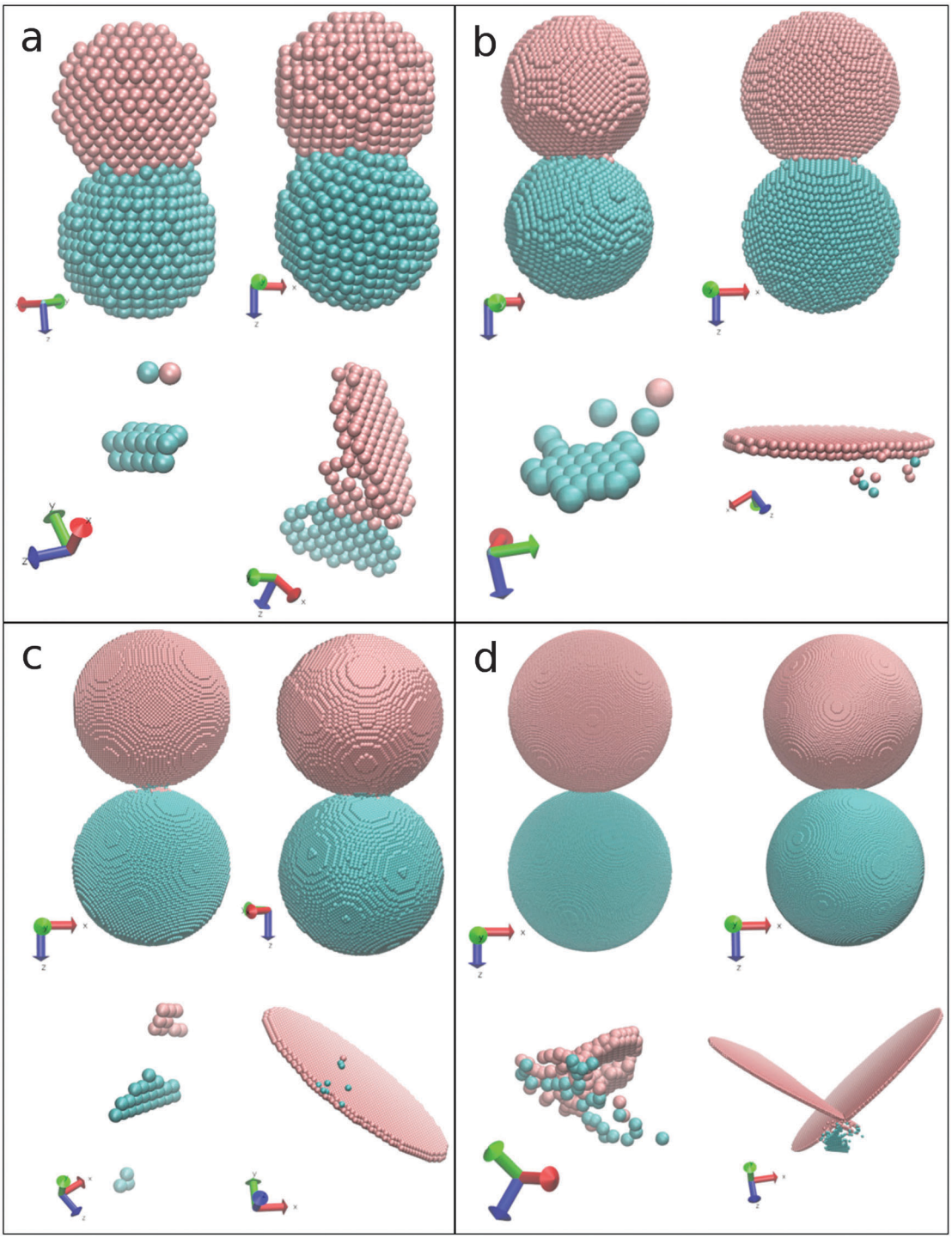

Fig. 2 Plasticity developing at the plastic threshold in the collision of two equal spheres. In each frame the top views provide a view on the collided system and show that the NP surfaces remain intact, while the bottom views present exclusively defect atoms – colored according to which NP the atoms belong – and reveal the defects generated in the interior of the NPs. (a) $N = 10^3$ atoms at velocity $v = 0.54$ (left) and $v = 0.56$ (right); $v_c = 0.55$. (b) $N = 10^4$ atoms at velocity $v = 0.35$ (left) and $v = 0.41$ (right); $v_c = 0.36$. (c) $N = 10^5$ atoms at velocity $v = 0.20$ (left) and $v = 0.25$ (right); $v_c = 0.24$. (d) $N = 10^6$ atoms at velocity $v = 0.10$ (left) and $v = 0.15$ (right); $v_c = 0.14$.

$v_c = 0.16$ based on eqn (1), caused in particular by the larger G – and hence yield strength Y – of crystals in this direction.

There exists no theory for the increase of v_c with decreasing R; however a number of models have been set up for related quantities. Thus several models have been set up for the rebound velocity, v_r, which measures the minimum velocity necessary for NPs to bounce off each other; at lower velocities they stick. The rebound velocity is thought to be related to the

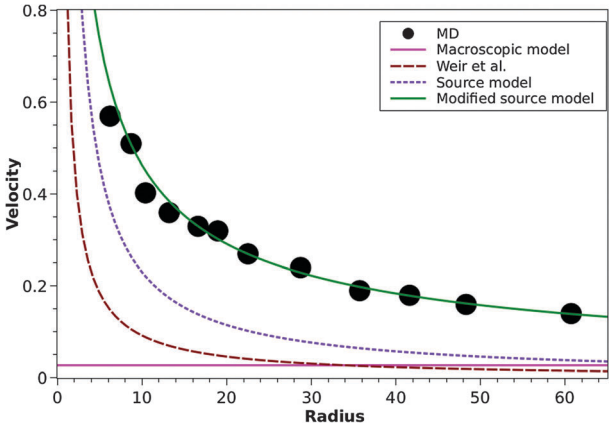

Fig. 3 Plastic threshold, v_c, as a function of NP radius, R. Symbols: our MD data. Lines provide available models: the macroscopic model, eqn (1), the model by Weir and McGavin, eqn (2), the simple source model, eqn (7), and our novel modified source model, eqn (9). The error in v_c is smaller than the symbol size.

critical velocity for plastic failure. Rennecke and Weber[53] provide measurements of v_r for Ag NPs with sizes between 10 and 100 nm rebounding from flat surfaces, and observed a strong increase of v_r with decreasing particle size R. They show that a model by Wang and Kasper,[54] which assumes completely elastic rebound, strongly underestimates the rebound velocity. However, the model by Weir and McGavin[55] is approached for the smallest particles sizes. This model assumes complete plastic failure during the contact and predicts rebound to occur above

$$v_r = \frac{\gamma}{\sqrt{3^{1/3} Y \rho}} \frac{1}{R}. \quad (2)$$

We use a value of $\gamma = 2.3$ for the surface energy of LJ crystals,[56] and the yield strength of $Y = 4$ and obtain in LJ units

$$v_r = \frac{0.92}{R}. \quad (3)$$

Other papers consider the size dependence of the coefficient of restitution; as soon as it starts deviating from values close to 1, they consider the NPs to have experienced increased energy dissipation which they attribute to the onset of plasticity. In this indirect way, Han *et al.*[32] showed that the onset of plasticity is shifted to higher velocities for smaller NPs. Takato *et al.*[27] followed this argument more systematically; they define the yield velocity v_y as the velocity, above which the rebound velocity stays constant (and hence the restitution coefficient decreases) and fitted their data to a size dependence as $v_y \propto R^{-0.65}$; however, no argument as to the specific functional form could be provided. For this study they use (100)-oriented LJ NPs; however atoms in different NPs interact purely repulsively in order to increase the rebound fraction to 100%.

C. Source models

We will consider here dislocation emission from the high-pressure contact region as the origin of plasticity. Inspired by the concept of the Frank–Read source,[47,57] we consider a dislocation to become emitted from the high-stress contact zone if the stress surpasses a value of

$$p_c = \alpha \frac{Gb}{R}. \quad (4)$$

In this simplest version of the source model we take the NP radius R as the relevant length; it defines the maximum radius of curvature that a dislocation line can acquire under the applied stress before it becomes unstable. The prefactor α has been determined by MD simulations for fcc crystals to be in the range of 0.25–1;[58,59] we use here $\alpha = 0.6$.

Since dislocation emission is governed by the applied stress, we need to convert the NP collision velocity v to pressure by using the Hugoniot relation, which relates the pressure p in a shocked material to the velocity of the piston driving the shock, u_p, and the velocity of the shock wave, u_s:

$$p = \rho u_p u_s = \rho v (c_l + s v) \cong \rho v c_l. \quad (5)$$

Here, the piston velocity has been identified with v, and the law $u_p = c_l + s u_p$ – with the longitudinal velocity of sound, c_l, and a constant s – valid for LJ solids[60] has been employed; for the small velocities present at the onset of plasticity, the equation has been linearized. For a LJ solid the longitudinal velocity of sound in the isotropic case is $c_l = \sqrt{(K + 4G/3)/\rho} = 10.52$, and eqn (5) reads

$$p = 11.41 v. \quad (6)$$

The simple source model, eqn (4) thus gives in LJ units $p_c = 26.25/R$ and hence

$$v_c = \frac{2.30}{R}. \quad (7)$$

This gives a $1/R$ dependence, similar to the Weir–McGavin model, eqn (2).

However, our MD simulations show that dislocations nucleate in the contact zone area, and hence the contact zone radius, a_c, should be used in eqn (4) rather than the entire NP radius. The physical picture here is the following: if a dislocation line of length $2a_c$ – spanning the contact area – has been generated, the high stress in the contact zone will drive it out into the NP, provided the line tension of the dislocation does not prevent it. At a critical stress of $\alpha Gb/a_c$ the dislocation will become unstable, leave the contact area and span the entire NP. Tanaka *et al.*[26] showed that the collisions of LJ NPs can be reasonably well described by the JKR theory of adhesive contact mechanics.[61] This theory determines the contact radius as

$$a_c = \left(\frac{9\pi w}{E_{ind}} R^2 \right)^{1/3}, \quad (8)$$

where $w = 2\gamma$ is the heat of adhesion. This formula is valid for zero external pressure; we use it to describe the contact radius at the time of dislocation nucleation. We checked for several cases in our simulations that the values obtained by eqn (8) represent the MD data well. In the simulation, at times beyond the dislocation nucleation, a_c further increases, and its final value at the end of the collision is – caused by the plastic

deformation—larger than the value given by eqn (8). When using a_c in the source model, we obtain $p_c = 16.4/R^{2/3}$ and

$$v_c = \frac{2.15}{R^{2/3}}. \quad (9)$$

In Fig. 3 we assemble our MD data for the critical velocity, v_c, and contrast it with the models described above. Note that in all these models, we did not use any fit factors to adapt to the MD data. The Weir–McGavin and the original source model show the wrong dependence on NP radius R; even if we introduced fit factors, they would not model the data. However the modified source model nicely fits the data in their $R^{-2/3}$ dependence; and even the quantitative agreement of the prefactor is surprisingly good. This also accounts for the previously unexplained result of Takato *et al.*[27] that gave an exponent of −0.65. We conclude that the modified source model adequately explains the elastic–plastic transition in NP collisions.

IV. Conclusions

In summary, our simulations show that the velocity – and hence the stress – necessary to generate dislocations in a NP increases with decreasing NP radius R proportional to $1/R^{2/3}$. Our data can be quantitatively modeled by our modified source model which assumes dislocations to be emitted from the contact area if the stress in the contact area becomes larger than the dislocation line tension. This model not only correctly reproduces the $1/R^{2/3}$ dependence of the critical velocity, but provides also a quantitatively correct description of the data obtained for the LJ NPs.

Already slightly above the critical velocity, volume-spanning planar defects (stacking-fault planes) are generated. The formation of nanotwins enclosed between pairs of SF planes is another typical outcome of the plastic activity slightly above the critical velocity.

These results have immediate consequences on the sticking and bouncing behavior of NPs since plasticity forms the dominant mode of energy dissipation in NPs. In addition, they influence the coefficient of restitution. The data presented here provides basic information to enter into granular-dynamics codes and is also relevant for nanotechnology applications using NPs, since plasticity can modify their properties.[62] Finally, as shown here, plastic slip leads to the generation of surface steps on the NPs, which may advantageously alter their properties for chemical processes such as, *e.g.*, catalysis.

In future work, the effect of non-central collisions needs be addressed as well as the peculiarities of specific materials that may not be well captured by the generic Lennard-Jones model. While metal clusters are of interest in basic research, collisions of quartz and water ice clusters are of immense relevance in astrophysics and planetary sciences. Finally it will be interesting to investigate how collisions between already collided (*i.e.*, pre-damaged) NPs differ from collisions of the single-crystalline clusters studied here.

Acknowledgements

E.M., D.T. and E.M.B. thank support from a SeCTyP project and PICT2009-0092. E.M. and D.T. acknowledge support from CONICET. H.M.U. has been supported by the Deutsche Forschungsgemeinschaft *via* Sonderforschungsbereich 926.

References

1 B. L. Holian and P. S. Lomdahl, *Science*, 1998, **280**, 2085.
2 C. Dominik and H. Nübold, *Icarus*, 2002, **157**, 173.
3 K. Wada, H. Tanaka, T. Suyama, H. Kimura and T. Yamamoto, *Astrophys. J.*, 2011, **737**, 36.
4 C. Ringl, E. M. Bringa, D. S. Bertoldi and H. M. Urbassek, *Astrophys. J.*, 2012, **752**, 151.
5 J. Duran, *Sands, powders, and grains: an introduction to the physics of granular materials*, Springer Verlag, 2000.
6 A. Gáspár, G. H. Rieke and Z. Balog, *Astrophys. J.*, 2013, **768**, 25.
7 A. E. Glassgold, J. Najita and J. Igea, *Astrophys. J.*, 2004, **615**, 972.
8 A. Chokshi, A. G. G. M. Tielens and D. Hollenbach, *Astrophys. J.*, 1993, **407**, 806.
9 C. Thornton and Z. Ning, *Powder Technol.*, 1998, **99**, 154.
10 V. Juvé, A. Crut, P. Maioli, M. Pellarin, M. Broyer, N. Del Fatti and F. Vallée, *Nano Lett.*, 2010, **10**, 1853.
11 K.-I. Saitoh and Y. Yonekawa, *J. Adv. Mech. Des. Syst. Manuf.*, 2010, **4**, 405.
12 J. Sun, L. He, Y.-C. Lo, T. Xu, H. Bi, L. Sun, Z. Zhang, S. X. Mao and J. Li, *Nat. Mater.*, 2014, **13**, 1007.
13 D. Mordehai, M. Kazakevich, D. J. Srolovitz and E. Rabkin, *Acta Mater.*, 2011, **59**, 2309.
14 D. Chrobak, N. Tymiak, A. Beaber, O. Ugurlu, W. W. Gerberich and R. Nowak, *Nat. Nanotechnol.*, 2011, **6**, 480.
15 D. Jang, X. Li, H. Gao and J. R. Greer, *Nat. Nanotechnol.*, 2012, **7**, 594.
16 A. Sedlmayr, E. Bitzek, D. S. Gianola, G. Richter, R. Mönig and O. Kraft, *Acta Mater.*, 2012, **60**, 3985.
17 L. M. Hale, D.-B. Zhang, X. Zhou, J. A. Zimmerman, N. R. Moody, T. Dumitrica, R. Ballarini and W. W. Gerberich, *Comput. Mater. Sci.*, 2012, **54**, 280.
18 A. Tolvanen and K. Albe, *Beilstein J. Nanotechnol.*, 2013, **4**, 173.
19 N. Pradeep, D.-I. Kim, J. Grobelny, T. Hawa, B. Henz and M. R. Zachariah, *Appl. Phys. Lett.*, 2007, **91**, 203114.
20 Y. T. Zhu, X. Z. Liao and X. L. Wu, *Prog. Mater. Sci.*, 2012, **57**, 1.
21 V. A. Lubarda, *Int. J. Plast.*, 2011, **27**, 181.
22 Y. Tang, E. M. Bringa and M. A. Meyers, *Acta Mater.*, 2012, **60**, 4856.
23 C.-C. Chen, C. Zhu, E. R. White, C.-Y. Chiu, M. C. Scott, B. C. Regan, L. D. Marks, Y. Huang and J. Miao, *Nature*, 2013, **496**, 74.
24 H. Zheng, A. Cao, C. R. Weinberger, J. Y. Huang, K. Du, J. Wang, Y. Ma, Y. Xia and S. X. Mao, *Nat. Commun.*, 2010, **1**, 144.

25 H. Kuninaka and H. Hayakawa, *Phys. Rev. E: Stat., Nonlinear, Soft Matter Phys.*, 2009, **79**, 031309.
26 H. Tanaka, K. Wada, T. Suyama and S. Okuzumi, *Prog. Theor. Phys. Suppl.*, 2012, **195**, 101.
27 Y. Takato, S. Sen and J. B. Lechman, *Phys. Rev. E: Stat., Nonlinear, Soft Matter Phys.*, 2014, **89**, 033308.
28 M. M. Mariscal, S. A. Dassie and E. P. M. Leiva, *J. Chem. Phys.*, 2005, **123**, 184505.
29 M. Kalweit and D. Drikakis, *Phys. Rev. B: Condens. Matter Mater. Phys.*, 2006, **74**, 235415.
30 N. Ohnishi, E. M. Bringa, B. A. Remington, G. Gilmer, R. Minich, Y. Yamaguchi and A. G. G. M. Tielens, *J. Phys.: Conf. Ser.*, 2008, **112**, 042017.
31 S.-C. Jung, J.-G. Bang and W.-S. Yoon, *J. Aerosol Sci.*, 2012, **50**, 26.
32 L. B. Han, Q. An, S. N. Luo and W. A. Goddard III, *Mater. Lett.*, 2010, **64**, 2230.
33 A. Michels, H. Wijker and H. K. Wijker, *Physica*, 1949, **15**, 627.
34 J.-P. Hansen and L. Verlet, *Phys. Rev.*, 1969, **184**, 151.
35 J. O. Hirschfelder, C. F. Curtiss and R. B. Bird, *Molecular theory of gases and liquids*, Wiley, New York, 1967.
36 D. T. W. Lin and C.-K. Chen, *Acta Mech.*, 2004, **173**, 181.
37 T. Halicioglu and G. M. Pound, *Phys. Status Solidi A*, 1975, **30**, 619.
38 P. Guan, D. R. Mckenzie and B. A. Pailthorpe, *J. Phys.: Condens. Matter*, 1996, **8**, 8753.
39 T. Hatano, *Phys. Rev. Lett.*, 2004, **93**, 085501.
40 D. Tanguy, M. Mareschal, P. S. Lomdahl, T. C. Germann, B. L. Holian and R. Ravelo, *Phys. Rev. B: Condens. Matter Mater. Phys.*, 2003, **68**, 144111.
41 S. Plimpton, *J. Comput. Phys.*, 1995, **117**, http://lammps.sandia.gov/.
42 W. Humphrey, A. Dalke and K. Schulten, *J. Mol. Graphics*, 1996, **14**, 33.
43 A. Stukowski, *Modell. Simul. Mater. Sci. Eng.*, 2010, **18**, 015012, http://www.ovito.org/.
44 A. Stukowski and K. Albe, *Modell. Simul. Mater. Sci. Eng.*, 2010, **18**, 085001.
45 A. Stukowski, V. V. Bulatov and A. Arsenlis, *Modell. Simul. Mater. Sci. Eng.*, 2012, **20**, 085007.
46 A. Stukowski, *Modell. Simul. Mater. Sci. Eng.*, 2012, **20**, 045021.
47 J. P. Hirth and J. Lothe, *Theory of dislocations*, Wiley, New York, 2nd edn, 1982.
48 W.-Z. Han, L. Huang, S. Ogata, H. Kimizuka, Z.-C. Yang, C. Weinberger, Q.-J. Li, B.-Y. Liu, X.-X. Zhang and J. Li, *et al.*, *Adv. Mater.*, 2015, **27**, 3385.
49 R. M. Davies, *Proc. R. Soc. London, Ser. A*, 1949, **197**, 416.
50 K. L. Johnson, *Contact mechanics*, Cambridge University Press, Cambridge, 1985.
51 D. J. Quesnel, D. S. Rimai and L. P. DeMejo, *Phys. Rev. B: Condens. Matter Mater. Phys.*, 1993, **48**, 6795.
52 A. Kelly and N. H. Macmillan, *Strong Solids*, Clarendon Press, Oxford, 3rd edn, 1986.
53 S. Rennecke and A. P. Weber, *J. Aerosol Sci.*, 2013, **58**, 135.
54 H.-C. Wang and G. Kasper, *J. Aerosol Sci.*, 1991, **22**, 31.
55 G. Weir and P. McGavin, *Proc. R. Soc. London, Ser. A*, 2008, **464**, 1295.
56 J. Q. Broughton and G. H. Gilmer, *Acta Metall.*, 1983, **31**, 845.
57 M. A. Meyers and K. K. Chawla, *Mechanical behavior of materials*, Cambridge University Press, Cambridge, 2nd edn, 2010.
58 V. B. Shenoy, R. V. Kukta and R. Phillips, *Phys. Rev. Lett.*, 2000, **84**, 1491.
59 A. K. Nair, E. Parker, P. Gaudreau, D. Farkas and R. D. Kriz, *Int. J. Plast.*, 2008, **24**, 2016.
60 T. C. Germann, B. L. Holian, P. S. Lomdahl and R. Ravelo, *Phys. Rev. Lett.*, 2000, **84**, 5351.
61 D. Maugis, *Contact, adhesion and rupture of elastic solids*, Springer, Berlin, 2000.
62 H. Portales, N. Goubet, L. Saviot, S. Adichtchev, D. B. Murray, A. Mermet, E. Duval and M.-P. Pileni, *Proc. Natl. Acad. Sci. U. S. A.*, 2008, **105**, 14784.